LHCb Silicon Tracker note 2002-061

The LHCb Inner Tracker cooling balcony and plate: Design and Material selection studies

Kurt Bösiger, Frank Lehner, Matt Siegler[1] and Stefan Steiner
University of Zurich, Switzerland

Jerzy Michalowski, Marek Stodulski and Pawel Zychowski
The Henryk Niewodniczanski Institute of Nuclear Physics, Cracow, Poland

Abstract

This internal note presents the design and the specifications for the cooling balconies and cooling plate of the LHCb Inner Tracker Silicon Detector. We describe the material R&D programme, which has been carried out in order to identify appropriate material candidates. Mechanical and thermal measurements on these materials are presented.

1 Introduction

The LHCb Inner Tracker will be made out of silicon microstrip detectors having a pitch of 198 μm. The complete tracking system will consist of three tracking stations each (IT1, IT2 and IT3) with four silicon strip detection planes in 0°, ±5° and 0° orientation. Every IT station has four detector boxes or enclosures which are arranged in a cross shaped way around the beampipe and are housing up to 28 silicon ladders each. A description of the layout of the LHCb Inner Tracker stations can be found in [1]. The design of the IT1-IT3 detector boxes is described in [2].

The basic building units of the detector are silicon ladders with either a 110 mm (one sensor) or 220 mm (two sensors) long and 78 mm wide area. The complete ladder is supported by a U-shaped carbon fiber composite made out of a high thermal conductive fiber material so that the carbon shelf under the silicon acts as a head spreader to give a lower temperature gradient along the silicon sensors. More details on the mechanical and thermal properties of the ladder support can be found in [3].

The carbon fiber support including the silicon sensors is mounted onto a cooling balcony piece using precisely machined holes and guide pins as reference features. These cooling balconies provide a mounting surface for the ladders in order to attach the ladders to a common cooling plate on top of a station quadrant, where a liquid coolant (C_6F_{14}) is circulated [4].

In the following, we report on the design and specifications of the balcony and cooling plate for the LHCb IT stations. Both parts have to fulfil structural, thermal, electrical and alignment purposes for the IT detector. The material

[1]Summer student from Cornell University, USA

candidates, which are appropriate for our cooling parts require therefore a high thermal conductivity, sufficient flexural strength, a low electrical resistance and machinability of the mechanical features for positioning and aligning. One of the most important criteria however, is the material budget of the detector. The involved materials must not deteriorate the designed momentum resolution of the tracker and therfore materials have to be selected that have radiation length X_0 and the hadronic interaction length Λ as small as possible. This note presents the current status of our material selection and characterisation studies, initiated in order to identify and qualify appropriate materials for cooling plate and balconies. The material selection program is not yet finished, as we have not completed the full characterisation measurements. However, the first preliminary results indicate which materials are suited as a baseline choice for the IT detector.

2 Cooling balcony and cooling plate design

2.1 Balconies

In the current design of the Inner Tracker, all silicon ladders of a box are mounted onto a common cooling plate via $66 \times 46 \times 1.5$ mm^3 large L-shaped balconies. The balconies provide mounting and alignment features by guide pins and establish a thermally conductive path from the cooling plate to the carbon fiber support and hybrid ceramic, which carries the front-end electronics on a kapton flex circuit. The mounting of the carbon fiber support and the hybrid ceramics onto the balcony happens through M1.6 screws. The alignment of the ladder reference system to the balcony system is established through guide pins of 1.5 mm diameter. The ladder assembly and alignment procedure is described in reference [5].

The mounting surface of the balconies has either a 0° or a ±5° orientation to the vertical direction depending on the silicon layer. Therefore we employ a total of three types of balconies: one for the 0° and two for the ±5° orientated ladders within one detector box.

Figure 1 shows the technical drawing of the 0°-balcony only. The mechanical specifications are

- machinability of precision holes 1P6 and 1.5P6 with their defined tolerances of $^{-14}_{-7}$ μm
- hole-hole distance of 50 ± 0.005 mm, other tolerances ±0.02 mm
- parallelism between indicated lines A of 0.005 mm
- perpendicularity between the two indicated surfaces B of 0.010 mm
- surface roughness of indicated planes shall be N8 (milled) and polished (N5)
- for other dimensions standard ISO-tolerances (ISO-2768) apply

The appropriate balcony material requires a high thermal conductivity. A finite-element analyses [6], which was carried out in order to investigate the cooling principle of the ladder concept revealed, that for the given balcony cross section, the thermal conductivity in direction of the heat transfer from the front-end electronics to the cooling plate should be larger than 150 W/m·K. This requirement will avoid too large temperature drops of more than 2 K along the balcony.

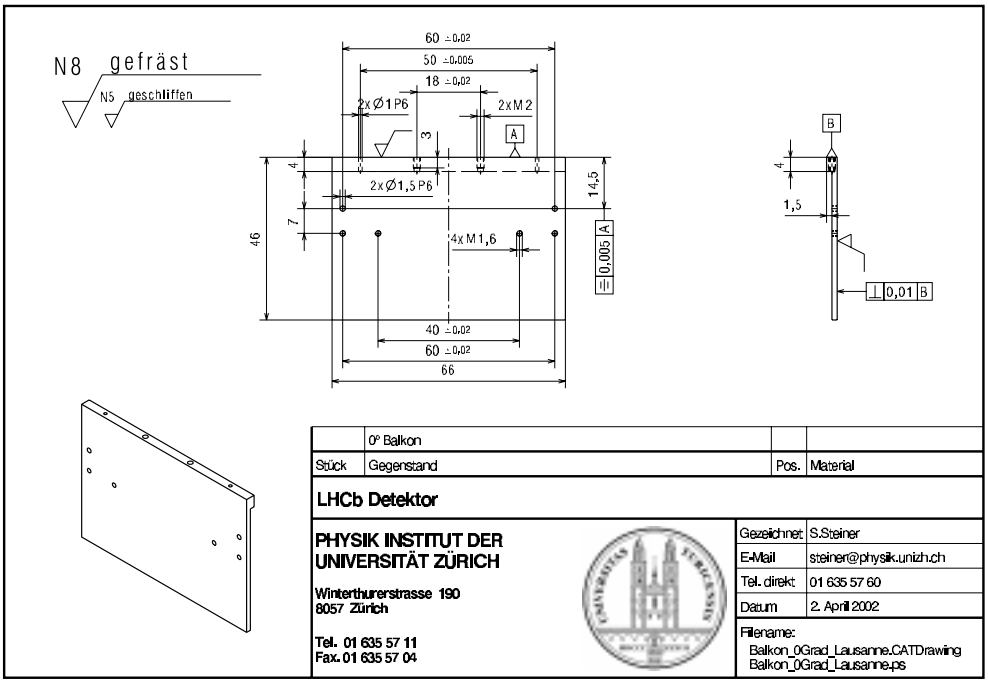

Figure 1: Technical drawing of the 0° balcony.

The thermal conductivity transverse to this direction is not so critical, since the heat flow is primarily in one dimension only.

In order to use the cooling plate as a common ground reference for all ladders within a box, the balconies have to be electrical conductive, since they will connect this common ground point to the signal ground on the ladder hybrid.

3 Cooling plate

The $564 \times 60 \times 2$ mm^3 large cooling plate provides a common mounting surface for all ladders of an IT box. A mechanical drawing of the cooling plate is shown in figure 2. The mechanical specifications of the plate require the machinability of 1H7 holes with their defined tolerance fields, since the ladders will be aligned on the cooling plate by means of two guide pins having 1 mm diameter. The overall flatness of the plate should be less than 0.2 mm over the full length. The cooling plate has seven threaded rods made out of a rigid polymer, which are used to mount a stiff honeycomb sandwich plate against the cooling plate. This structure will give enough bending resistance and minimise the deflection of the cooling plate under the mechanical load of 28 ladders. A first finite element analysis showed, that the local deflection of the cooling plate is limited to less than 20 μm, if the cooling plate is supported rigidly at seven points. This preliminary study is based on the flexural strength of Aluminium. However, more finite-element investigations and deflection measurements, which can be carried out on our metrology machine are necessary to confirm this numbers.

The cooling plate is surrounded by a cooling pipe to circulate a coolant at -15°C. The cooling plate acts as uniformly cold horizontal surface with an aimed

plate temperature of around -10°C, so that convective processes inside the box can cool the inner box ambient down to $T_{box} = 0 - 5°C$ [2]. Since a full heat load of up to 75 W per Inner Tracker box is expected [4], the plate material requires a low thermal impedance to limit the temperature drop from the cooling pipe wall to the cooling plate of below 5 K. The thermal resistance of the first cooling plate prototype made out of 1.5 mm thick aluminium was measured to be 0.11 K/W [2], i.e. almost 8 K instead of the hoped 5 K. However, a thicker cooling plate would theoretically reduce this resistance on the expense of increasing the material budget.

We therefore require the thermal conductivity of the cooling plate material as high as aluminium by having a high radiation length of the material as well. We believe that due to the design of the cooling plate and the embedded cooling pipes, the thermal conductivity of the material does not need to be isotropic. It is probably sufficient to have a very high conductivity parallel to the short side of the plate, in order to remove the heat from the balconies to the cooling pipe in a direct way. These assumptions however, have to be verified by additional FEA calculations.

The electrical resistance of the cooling plate material should be very low, since we define the star-point of the grounding through it. A further requirement of the cooling plate material is a high specific stiffness (strength divided by density) and more important, also a high value of E/ρ, where E is the Young's modulus. The last requirement is necessary since the effects of vibration due to the turbulent running of the cooling fluid have to be minimised. A finite-element analysis FEA analysis and measurements to investigate this effect are in preparation.

4 Overview of material candidates

This section reports on the various kinds of materials, which we have considered as potential candidates for balconies and cooling plate. For each material, we compare the main mechanical properties, the thermal properties and the rough costs. Since the materials are used for thermal and structural applications and a high radiation length is of utmost importance for the achieved momentum resolution of the detector, we have decided to compare further derived quantities as well: $\lambda \cdot X_0$, $E \cdot X_0$ and $E \cdot \lambda$.

4.1 Metals

We have fabricated first prototype balconies and the cooling plate out of Aluminium. The thermal and mechanical properties of Aluminium are satisfactory. The low radiation length of Aluminium however, is a concern. That is why we have pursued for some time two other metal options as well: Beryllium and AlBeMet. Beryllium has the big advantage of having a very high radiation length. AlBeMet is an alloy containing as weight fraction 62% Beryllium and 38% Aluminium. Since Beryllium and Beryllium-containing alloys are toxic, very restrictive safety measures are applied, making the machining costs very expensive[2] in addition to

[2]We have asked two companies (Avimo, UK and HERAEUS, Germany) for quotes on Beryllium or AlBeMet machined balconies. The costs would be between 450-700 CHF/pc and are considered by far

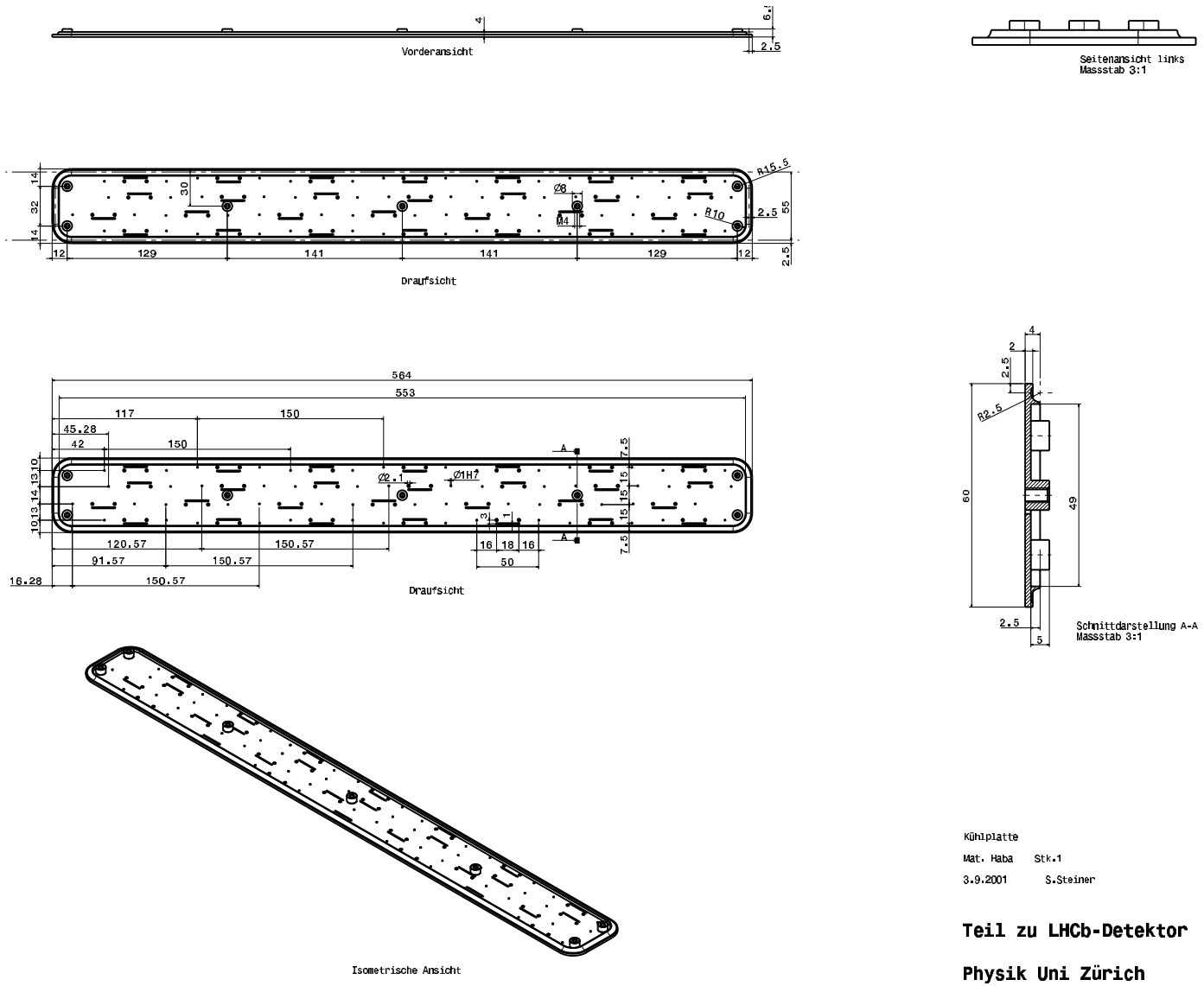

Figure 2: Technical drawing of the cooling plate.

Table 1: Some metal properties which are of interest. We have specified the detailed metal alloy, which would be used for our application in order to have a fair comparison. The costs are estimates based on a survey.

Material	Al (6061)	AlBeMet (AM 162)	Be (SR200)	Mg (AZ91)
density ρ (g/cm^3)	2.75	2.1	1.85	1.81
E-module (GPa)	69	193	303	45
Tensile Strength (MPa)	570	262	480	250
λ (W/mK)	150-190	210	200	72
CTE (10^{-6} 1/K)	23.6	13.9	11.5	25
Radiation length (cm)	8.9	16.1	35.3	13.1
hadr. interaction length (cm)	39.4	39.7	40.6	50.4
raw material cost CHF/kg	3	800	1500	5

the already very high raw material costs. Although the usage of Beryllium and its alloys is allowed at CERN [7], it is more and more recommended to limit its usage to the absolute minimum.

Table 1 compares the main properties of the aforementioned metals. We have added Magnesium, since it will have importance in the further discussion of Metal-Matrix Composites in the next section.

4.2 Metal matrix composites

Metal matrix composites (MMC) consist of a metal matrix reinforced with ceramic or metallic particulates or fibers. This class of composite materials is often used in aerospace and automobile industry due to their exceptional characteristics [8], such as high specific strength and stiffness. In particular, carbon fiber-reinforced Aluminium and Magnesium composites receive currently considerable scientific and industrial interest as a result of their excellent physical properties.

The advantages of MMC materials over metals are a lower CTE which can be almost near zero, leading to good dimensional stability control, a better specific modulus and a lower density. Compared to polymer matrix composites, MMCs do not absorb moisture and exhibit a much better behaviour at higher temperatures. Moreover, they give better transverse and longitudinal thermal conductibility than standard fiber reinforced polymers because of the underlying metal matrix. From the design and construction point of view, the machinability of MMCs can be well controlled and mounting and joining of MMC pieces represent no difficulties.

In order to study the suitability of MMC materials for our balconies and cooling plates, we have approached the Swiss Federal Research Institute EMPA in Thun. This institute has a dedicated and experienced material research group, which is focusing on R&D for MMC industrial applications.

For our application purposes MMC are promising candidates, since they combine the strength of an uniform metal matrix with superior thermal properties of special carbon fiber materials. It was decided to produce three MMC sam-

too high.

ples in a special squeeze casting process at EMPA at temperatures of 700°C in an inert atmosphere. Magnesium was chosen as a metal matrix due to its lower radiation length than Aluminium and its excellent casting properties. By embedding carbon or graphite based material into a Magnesium matrix, the radiation length of the composite will be further enhanced compared to pure Magnesium. To our knowledge this is the first MMC study focusing on a very high thermal conductivity.

The preferred Magnesium alloy for the squeeze casting is AZ91HP containing 9%-wt Al and 91%-wt Mg. This high purity alloy has a very low content ($< 0.01\%$) of Fe, Cu and Ni so that corrosion effects are minimised. As a reinforcement we have chosen three different materials:

- continuous carbon fibers, Cytec Thermalgraph 6000X
- discontinuous carbon fibers, Cytec chopped fibers DKDX
- graphitic foam, Oak Ridge National Laboratory

The continuous fibers Cytec Thermalgraph 6000X[3] are pitch-based, long oriented fibers pressed to a panel with a very high bulk thermal conductivity of 550 W/mK. The solid panels do not contain any binder material and are well-suited for infiltration purposes. However, they are rather brittle and can not be machined without reinforcement material. The fibers are very similar in properties to the Amoco K800 and K1100 fibers[4]. Panels with 20-30% higher density are principally available and would enhance the thermal conductivity even more.

The short or discontinuous fibers Cytec DKDX have an average filament size of 200 μm and exhibit high thermal conductivity between 400-700 W/mK as well. By infiltrating a chopped fiber preform with Magnesium, the unoriented short fibers in the matrix tend to give more uniform thermal and mechanical properties to the resulting MMC. However the final carbon fiber volume content of unoriented short fiber MMCs is typically much smaller than in the oriented case, so that big improvements in the radiation length and thermal conductivity are not expected. The chopped carbon fiber preform which was produced for the magnesium infiltration process consisted of 25%-vol. fiber material only.

The last MMC sample was made out of a 98% open cell graphitic foam, in which Magnesium was infiltrated. The graphitic foam was produced in the metal and ceramics division of Oak Ridge National Laboratory (ORNL) [9]. Since we found this newly developed graphitic foam to be a very interesting and promising material candidate, we started an own characterisation program. More details of the graphitic foam can be found in the next section.

All three MMC samples have been tested with respect to their thermal and mechanical properties. Out of the three infiltrated samples, balconies were machined at EMPA according to the specifications in the technical drawing of figure 1. A photograph of the three machined MMC balconies is shown in figure 4. The machinability and quality of the threads and precision holes were visually inspected. The results of the measurements together with the results from the other material candidates are summarised in section 5.3.

[3]Cytec Industrials, USA

[4]Cytec corporation has recently purchased the carbon fiber department of Amoco BP

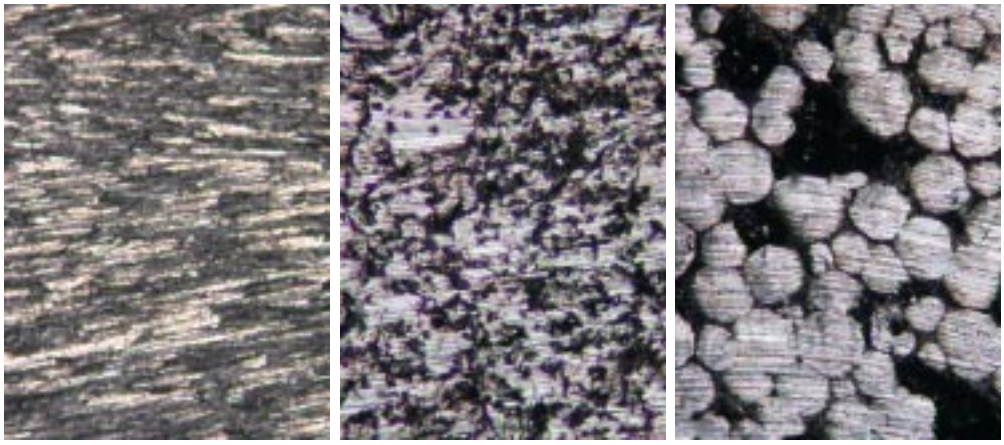

Figure 3: Microscopic close-up of the three MMC samples. Left: The long fiber MMC. Middle: The MMC material with short fibers. Right: The MMC with graphitic foam.

4.3 Graphitic foam

A special graphitic foam with a high thermal conductivity has been developed in the Metals and Ceramics division of Oak Ridge National Laboratory (ORNL) [9]. The foam is fabricated from a mesophase pitch-based precursor material by a special blowing technique resulting in an 98% open cell structure with highly aligned cell walls of a graphitic structure leading to a relatively high bulk thermal conductivity of more than 100 W/mK for such a low density material. The mean pore diameter of the foam is in the order of 100 μm. Due to the interconnected network of graphitic ligaments, the foam material exhibits nearly isotropic material properties. That is why the foam seems to be a very good candidate for a potential reinforcement phase for structural composite materials which require thermal conductivity.

The thermal conductivity of the foam depends strongly on the precursor material and the final foam density. The larger the foam density is, the higher the thermal conductivity of the foam. Typically, the standard foam densities are between 0.5-0.7 g/cm^3, but higher density foam can be produced.

We have received several foam samples from ORNL. A lower density foam sample was infiltrated with Magnesium at the EMPA/Thun as described in the previous section. The other foam samples had various densities and were produced by ORNL specially for us. The graphitic foams could be densified by carbon vapor infiltration (CVI) methods, reaching final densities of up to 1.13 g/cm^3.

Another type of graphite foam is commercially produced by the company Mercorp, USA. We have measured on one sample from this company the thermal conductivity and have included it in our comparisons.

Some of the foam samples have been encapsulated in an epoxy or cyanate ester resin. This infiltration was done by vacuum suction. We have machined balconies out of those foams in order to evaluate the machinability and to measure the thermal conductivity directly on final machined balconies. The radiation length of graphitic foams are very high, since the material has a low density.

4.4 Carbon-carbon composites

The option to realize the cooling plate based on a carbon-carbon (C-C) composite is being pursued as well. The high energy physics detector group at the Institute for Nuclear Physics in Cracow was therefore approached. The group has much experience in carbon composite materials and has built several C-C prototype supports for the ATLAS pixel detectors.

Because of the fast turn-around times of Toray M55J carbon fiber fabrics, a first series of C-C prototype plates in a special carbonisation process at high temperatures done at the institute in Cracow was produced. The starting carbon fiber fabrics itself does not posses a very high thermal conductivity, but is well suited for first evaluation studies and measurements. Especially, the question has to be addressed if C-C material mechanically qualifies as cooling plate material and how the joints between an embedded cooling pipe and the C-C plate with small thermal resistances can be designed.

In the meantime, Cracow has fabricated the first sample of a C-C plate and another composite sample having the M55J carbon fiber tissue in a phenolic resin. The thermal conductivity, the Youngs' modulus and the tensile strength on these plates were measured.

5 Material Characterisations

5.1 Thermal measurements

We have set up a cooling test stand at the University of Zurich to measure the thermal conductivity of machined balconies in-situ. The right photograph of figure 4 shows a cooling block made our of copper, which carries a cooling pipes for water cooling. The balcony is mounted on the cooling block by two M2 screws, as it is foreseen in the final Inner Tracker detector design. We have used a silicone based thermal joint[5] to enhance the thermal contact of the interface. The balconies had at the far end small Kapton heater elements[6]. Three temperature sensors[7], which have been attached on the balconies by using a very thin double-adhesive film measured the temperature profile directly along the balcony between heater element and heat sink. The setup was placed inside a small thermally insulating enclosure with a dry air purging to avoid condensation. The temperatures on the cooling block and inside the insulating box were also recorded. We have avoided a too high temperature difference between balcony and ambient, in order to minimise convective effects.

We have measured the temperature profile on the balcony for up to 10 different power settings on the kapton heaters varying from 0 W to 5 W. In each run, the gradient of the measured temperature versus the distance from the cooling chuck was calculated and finally the thermal conductivity was determined by a linear fit to the temperature gradients as function of the applied power.

[5] Wakefield Engineering silicone compound, 120 Series
[6] Minco Kapton heater, $R = 10.5\Omega$
[7] Dallas Semiconductor DS18S20

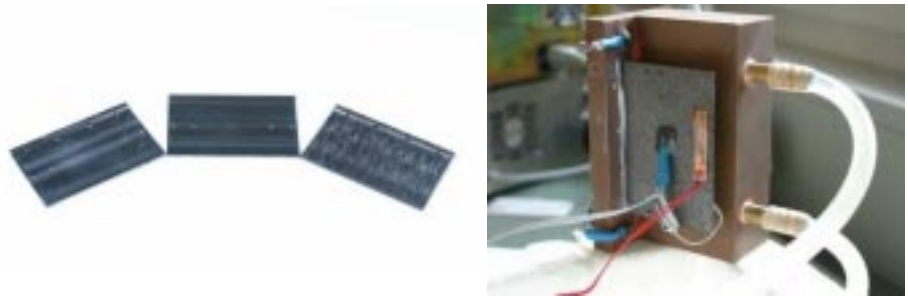

Figure 4: Left: (Courtesy of EMPA, Thun) Photograph of the three machined MMC balconies using graphitic foam (left), short fibers (middle) and continous fibers (right). Right: Picture of the laboratory setup for the balcony cooling tests.

The two graphs in figure 5 present typical results of the measurements. The balcony material was Magnesium with short fibers. The upper plot shows the recorded temperatures at three different heater settings as a function of the distance from the cold chuck. The more power Q is dissipated by the heater, the steeper the slope is, if the cold chuck is kept cold. By determining the slopes and knowing the cross sectional area A of the balcony, we can simply extract the thermal conductivity λ of the materials.

$$Q/A = \lambda \cdot \Delta T/\Delta x \tag{1}$$

The lower plot in figure 5 gives the measured $\Delta T/\Delta x$ data points as a function of the power settings. The data points are described nicely by a linear curve as expected from the conductive heat transfer.

In order to verify if our results are consistent we have measured an Aluminium alloy (AlMgSi or Al 6061) balcony as reference. The determined value of the thermal conductivity was 177 W/mK and fits very well into to given span of quoted values for Aluminium 6061 in table 1. In addition, several material specimens of standard size $5 \times 5 \times 35$ mm^3 were prepared in order to evaluate the thermal conductivity at the Fraunhofer Institute for ceramic technologies and sinter materials (FhG-IKTS) using a certified comparative method. The claimed uncertainties at the FhG-IKTS are less than 5% for thermal conductivities of less than 250 W/mK. For higher values of the thermal conductivity only a lower limit could be set. The thermal conductivities of the materials, which have been measured at the FhG-IKTS and by us with the in-situ balcony measurement method are consistent with each other on a 10-15% level.

5.2 Mechanical Measurements

We have machined material samples to a standard size rod of $5 \times 5 \times 50$ mm^3 for further mechanical characterisations. The E-modulus and the ultimate tensile strength was determined from a tension test. The tension test was carried out at EMPA Dübendorf and partially at the Institute for welding techniques (SLV) Munich with a Zwick universal testing machine allowing an applied force of up to 20 kN. For the C-C sample, the mechanical tests were done at Cracow.

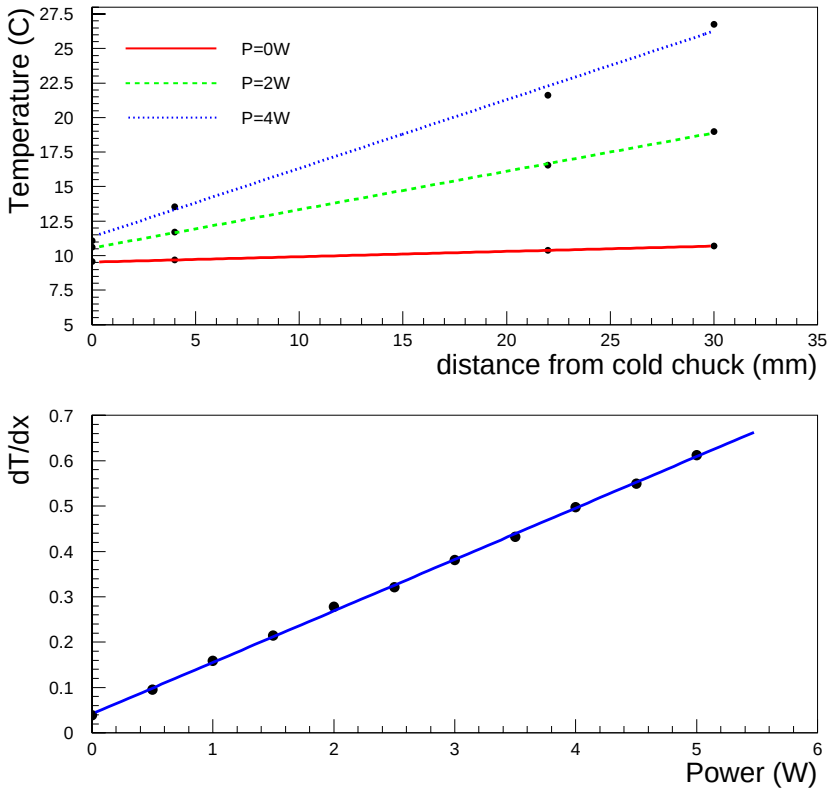

Figure 5: Measurement of the thermal conductivity on the Magnesium and short fiber MMC. The upper plot shows the measured temperature data for different power settings as function of the distance to the cold chuck. The lower plot presents the temperature slopes as function of the power.

Table 2: The different material samples, which have been investigated.

Sample name	**Comments**	**Machinability**
Mg MMC with long fibers (MgLF)	-	good
Mg MMC with short fibers (MgSF)	-	very good
Mg MMC with graphitic foam (MgGF)	-	holes and threads medium quality
Thermalgraph long fiber (LF)	-	very poor, machining impossible
Graphitic foam (ORNL 1a)	sample with low density $\rho = 0.39$ g/cm^3	poor, machining of threads and precision holes impossible
Graphitic foam (ORNL 1b)	sample with low density encapsulated with epoxy	machining of threads acceptable
Graphitic foam (ORNL 2)	sample with medium density $\rho = 0.57$ g/cm^3	poor, machining of threads and precision holes impossible
Graphitic foam (ORNL 3)	sample with high density $\rho = 0.815$ g/cm^3	machining of threads and precision holes very difficult
Graphitic foam (ORNL 4)	sample with low density encapsulated with cyanate ester	machining of threads accepable
Graphitic foam (ORNL 5a)	sample with very high density encapsulated with epoxy	machining of threads acceptable
Graphitic foam (ORNL 5b)	sample with very high density $\rho = 1.13$ g/cm^3	machining of threads and holes medium to poor
Mercorp graphitic foam (Mercorp)	sample with low density	machining of encapsulated sample medium to poor
C-C from M55J tissue (Cracow 1)	sample produced & measured at Cracow	
M55J tissue in phenolic resin (Cracow 2)	sample produced & measured at Cracow	

5.3 Compilation of results

We present here the results of the evaluated samples. For a better overview, the sample names and further explanations and comments to the samples are listed in table 2. We have added a column in the table, which describes the machinability of the material with respect to the required precision holes and threads of the balconies. The machining quality of the holes and threads was checked by a visual inspection only.

Typically, the graphitic foam products with medium or low density could only be machined to balconies, if they are encapsulated in a matrix of epoxy or cyanate ester resin. Higher density foam like the ORNL 5a+b samples could principally be machined, but with rather bad quality of the precision holes and threads. An infiltration with epoxy improves the quality considerably.

The results of the thermal and mechanical tests are listed in table 3. Here, we compare the density ρ, Young's modulus, the strength, the thermal conductivity λ, the radiation length X_0 and the hadronic interaction length Λ of the samples. Unfortunately we do not have on all samples mechanical data available.

For the radiation length and the hadronic interaction length calculations of the composite materials, the 'rule of mixture' has been used:

$$1/X_0 \ (g/cm^2) = \sum_i w_i/X_0^i \tag{2}$$

The weight fractions w_i were calculated by measuring the densities of the

Table 3: The results on the material properties. The footnotes mean: (1) beyond limit of tension test, (2) measured at U of Zurich, (3) measured at FhG-IKTS, (4) information from manufacturer, (5) measured at Institute of Nuclear Physics in Cracow

Sample	ρ **(g/cm^3)**	**E-mod. (GPa)**	**Strength (MPa)**	λ **(W/mK)**	$\mathbf{X_0}$ **(cm)**	Λ **(cm)**
MgLF	2.05	1000-1400	$> 500^1$	433^2	17.1	43.5
MgSF	1.92	63	69.6	89^2, 78^3	16.0	47.7
MgGF	1.86	24.2	27.1	82^2, 76^3	15.4	50.5
LF	1.48	180-280	10.3	550-600^4	28.1	58.5
ORNL 1a	0.39	-	-	23.5^3	104	217
ORNL 1b	1.34	4.5	8.23	22.9^3	30.7	71.8
ORNL 2	0.57	0.23	0.1	47^3	72.2	150.6
ORNL 3	0.815	2.91	3.7	51^3	50.7	105.9
ORNL 4	1.26	-	-	43^2	32.7	78.1
ORNL 5a	1.39	-	-	128^2	29.8	63.9
ORNL 5b	1.22	0.31	1.6	250^2	36.5	76.1
Mercorp	1.23	0.7-3.5^4	1.2-20^4	48^2	33.4	78.2
Cracow 1	1.43	355^5	30^5	118^5	28.9	60.33
Cracow 2	1.52	497^5	28^5	117^5	27.2	61.3

composite materials having either graphite, magnesium, air or epoxy content with known X_0^i and Λ^i as tabulated[8] in the particle data book [10]

The assumed volume and/or weight fractions of the composites could be double-checked on the infiltrated materials (either with epoxy or magnesium). Here, we verified the composition by comparing the weight fractions from measured densities before and after infiltration.

5.4 Discussion of results

5.4.1 Mechanical results

The Young's modulus of the Magnesium MMC with long fibers shows a superior result, but the uncertainty in the measurement is rather high, which is indicated in the spread of the quoted values of table 3. The high modulus is a direct consequence of the longitudinal fibers in the reinforced magnesium matrix. However, the long fiber panel alone gave smaller values of the modulus. The reason of this is due to fixation problems during the testing, so that only small elongations were used for determining the modulus of the long fiber panel.

An improvement of the modulus was observed in the Magnesium MMC sample reinforced with short fibers. The modulus increased here from 45 GPa for AZ91 (see table 1) to 69 GPa. The usage of graphitic foam as a reinforcement material however, turned out to worsen the modulus from 45 GPa to 24.2 GPa.

Very high values for the modulus and the strength were achieved with the C-C sample and the M55J tissue reinforced with phenolic resin. Both plate prototypes

[8] We have used the quoted Λ-values in [10] for graphite and epoxy. For Magnesium we have calculated Λ according to $\Lambda(g/cm^3) = 35 \cdot A^{1/3}$, with A being the number of nucleons.

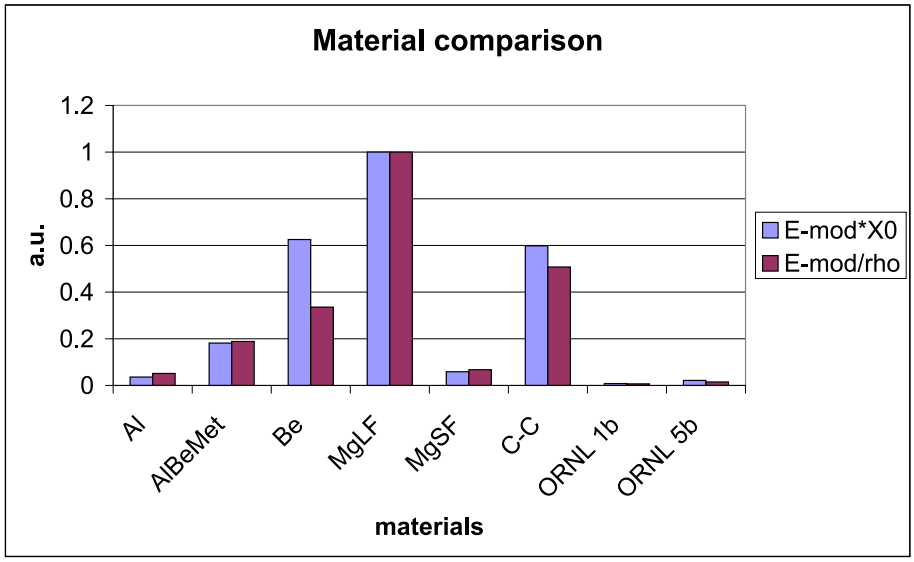

Figure 6: Relative comparison of the mechanical quantities $E \cdot X_0$ and E/ρ for eight selected materials. The values have been normalized to the value giving the highest $E \cdot X_0$ and E/ρ respectively. The materials are: Aluminium, AlBeMet, Beryllium, Magnesium MMC with long fiber, Magnesium MMC with short fiber, the carbon-carbon composite manufactured in Cracow and two ORNL graphitic foam samples.

were fabricated in Cracow and seem to be very promising cooling plate candidates. However, the machinability has not yet been tested.

It is clear, that graphitic foam in general can not reach the same dimensional stability as MMCs. In general, their E-modulus is dependent on the graphite orientation and more strongly, on the density of the foam. The medium density foam ORNL 2 gave already a value of 230 MPa for the modulus, which is an excellent number for carbon/graphite foam products [11] in that density range. For the highly densified foam ORNL 5b an E-modulus of 310 MPa was observed. One sample with an exceptional strength was foam ORNL 3 with a density of $\rho = 0.815$ g/cm^3. This sample yielded much higher values for the modulus and strength in the tensile test than the other foam samples. The reason for this is so far unknown.

The strength of the foam samples can be dramatically improved by epoxy infiltration. The epoxy infiltrated sample ORNL 1b, which is a low density graphitic foam, achieved a modulus of almost 5 GPa, i.e. a factor of 20 improvement. Here, the low-density foam was completely infiltrated with epoxy serving as a strong bonding matrix for the graphitic cell ligaments. In the case of denser foams, the infiltration process turned out to be more difficult and was possible only under vacuum suction. In the case of ORNL 5a+b, the epoxy infiltration was also incomplete, leaving around 15 vol-% of open graphitic cells in the sample after epoxy encapsulation. Hence, the improvement in the modulus and strength which was obtained for ORNL 5a after infiltration was a factor of 2 only.

In figure 6 we compare the mechanical quantities $E \cdot X_0$ and E/ρ for eight selected materials out of table 2. The quantities $E \cdot X_0$ and E/ρ can be used as a

figure of merit for selecting the candidate, which would perform best if used as a cooling plate material. A high modulus together with a high radiation length is a substantial requirement for the cooling plate. Moreover, the specific modulus E/ρ is important to minimise vibrational effects[9]

The material, which performs best in both categories is the Magnesium MMC with long fibers. However, the modulus has been measured on this material in the fiber direction only and we have to further characterise it in the transverse direction as well in order to finally decide if it is suited as cooling plate material. Another option for the cooling plate could be the carbon-carbon composite as it was produced in Cracow from a M55J tissue. It performs rather well in $E \cdot X_0$, but lacks of thermal conductivity. This is due to the used M55J carbon fiber in the weave used for the carbonisation process. It would be principally possible to produce C-Cs out of tissues consisting of a higher thermal conductive fiber material, but further prototyping studies with respect to the machinability and to solve the cooling pipe attachment issue, have to be carried out first.

5.4.2 Thermal Results

The thermal conductivity of 433 W/mK of the Mg MMC sample having the long fibers is very high along the fiber direction. This material seems to be the optimum choice for balconies, since the balconies require heat transfer in one direction only. Due to the volume fraction of 33% Magnesium in the sample, we expect a thermal conductivity transverse to the fibers of at least 30 W/mK. However, we have to verify this number by future measurements.

The thermal conductivity of the other two Magnesium MMC samples is essentially dominated by the Magnesium bulk matrix. At least in the MgSF case, we had hoped for an improved thermal conductivity due to the presence of the chopped fiber material.

In case of the graphitic foam materials we found, that the thermal conductivity generally increases towards higher density. The densification however, reduces the radiation length as it is shown in figure 7. In this graph we have plotted the results from the thermal measurements on the graphitic foams as a function of its density. The available data, although they are sparse, allow for this conclusion.

Since graphitic foams can only be considered as balcony candidates if they are encapsulated in a resin matrix, we have included the epoxy resin contribution from an infiltration in the radiation length calculations in order to obtain a more realistic picture.

The densified foams ORNL 5a and ORNL 5b have densities between $\rho = 1.13 - 1.22$ g/cm^3 (without infiltration) and yielded very high thermal conductivities of 128 W/mK and 250 W/mK respectively. Although both samples were subject to the same densification process, the overall foam quality is quite different and the better thermal conductivity result of ORNL 5b is probably due to better aligned cell wall structures. Our finding on the two delivered ORNL 5a+b samples was independently confirmed by the responsible ORNL engineer [12].

The thermal conductivity result of the densified ORNL 5b foam is very promising. The high density foam is a strong balcony material candidate as well, since

[9]The vibrations are roughly proportional to $\sqrt{\rho/E}$ due to the turbulent flow of C_6F_{14}.

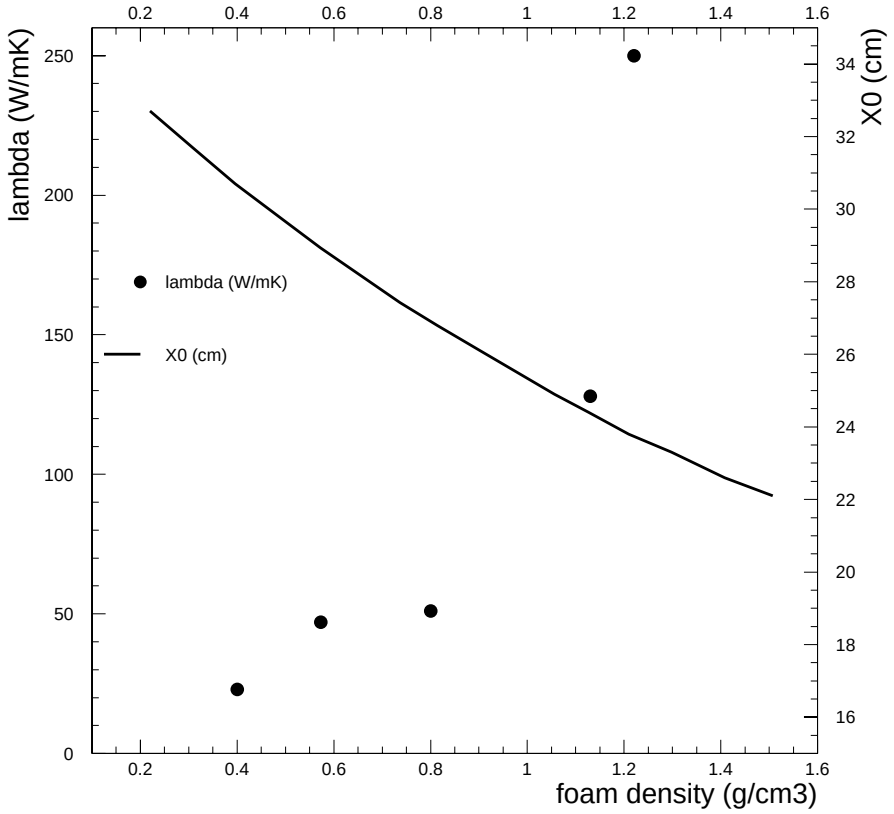

Figure 7: The measured thermal conductivities of the graphitic foam as function of its density. The solid line presents a X_0 calculation of the foams, assuming the foam is encapsulated with epoxy.

it gives the highest numbers of $\lambda \cdot X_0$, as shown in figure 8. In our opinion it is well worth to perform further studies on this material and to investigate other properties like CTE and modulus. However, we have to clarify how reliably such high density graphite foam can be produced at ORNL.

6 Conclusions

We have presented the design of the cooling balconies and cooling plate for the LHCb Inner Tracker Silicon detector. The mechanical and electrical specifications of the machined parts were discussed. A broad material R&D study is investigating the suitability of various materials including metals, metal matrix composites, carbon-carbon composites and graphitic foams.

We have launched a material development program on Magnesium based MMCs together with the EMPA Thun. The resulting long fiber Magnesium MMC gave very high thermal conductivity and a high E-modulus along the fibers. It is a very promising balcony and cooling plate material, but further studies on

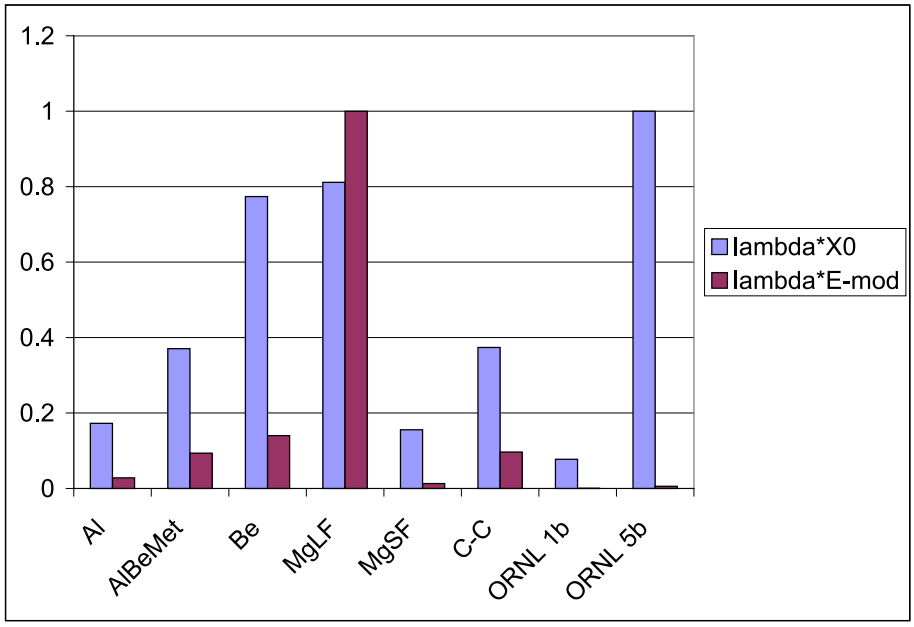

Figure 8: Relative comparison of the thermal quantities $\lambda \cdot X_0$ and $\lambda \cdot E$ for eight selected materials. The numbers have been normalized to unity. The materials are: Aluminium, AlBeMet, Beryllium, Magnesium MMC with long fiber, Magnesium MMC with short fiber, the carbon-carbon composite manufactured in Cracow and two ORNL graphitic foam samples.

the properties transverse to the fiber like thermal conductivity and E-modulus are necessary. These studies will be carried out in the near future and another prototype infiltration run is currently in preparation. If we decide to built both, balcony and cooling plate, out of the same material, then CTE mismatches are greatly avoided. The overall machining quality of this MMC material is good, but requires the usage of special diamonds tools, which eventually leads to a more time consuming production.

Another option for the balconies could be the high density graphitic foam as produced by ORNL. Due to machining constraints we can use this material only infiltrated with epoxy. The thread and precision hole quality seems to be acceptable. Nevertheless, it is rather likely, that the material does not possess the required bending strength to qualify as cooling plate material. In that case we have to use a combination of graphitic foam for the balconies and either MMC or a C-C composite material produced from a higher thermal conductive carbon fiber tissue at Cracow for the cooling plate.

7 Acknowledgement

We would like to thank Sebastien Vaucher from EMPA Thun for the realization of the MMC project at EMPA. We are greatly indebted to James Klett from Oak Ridge National Laboratory for providing us with several foam samples for the characterisation measurements.

References

[1] O. Steinkamp: Layout of a Cross-Shaped Inner Tracker, LHCb 2001-114

[2] K. Bösiger, F. Lehner, S. Steiner and S. Strässle, Design, Construction and Thermal Measurements on a Detector Box for the Inner Tracker of the LHCb Experiment, LHCb 2002-059

[3] R.J. Frei et al. Thermal and mechanical studies of the U-shaped carbon fiber support for the LHCb Inner Tracker detector's ladder, LHCb 2002-060

[4] F. Lehner and M. Stodulski: The liquid cooling system of the LHCb Inner Tracker: design constraints and considerations, LHCb 2002-066

[5] B. Carron et al., Assembly Procedure for the Silicon Inner Tracker, LHCb 2002-065

[6] J. Blocki and F. Lehner, Investigations of the thermal properties of the LHCb Inner Tracker silicon ladders by finite element analysis, LHCb 2001-128

[7] Beryllium Safety Instructions. CERN-TIS document 25

[8] F. Moll, Beanspruchsgerechte Verbundmetalle, Zeitschrift Werkstofftechnik SMM, 45-2000

[9] James Klett et al., High-Thermal-Conductivity, Mesopahse-Pitch-Derived Carbon Foams: Effect of Precursor on Structure and Properties, Carbon, 38(7), pp953-973 (2000)

[10] Review of Particle Physics, The European Physical Journal C, Vol 15, 2000.

[11] J.C. Withers and J.P. Patel, Processing and properties of graphite foams, 45th Internationsl SAMPE Symposium on carbon fibers and novel carbon fiber applications, May 21-25, 2000.

[12] J. Klett, ORNL, private communication